Adsorption of NH_3 and H_2O in Acidic Chabazite. Comparison of ONIOM Approach with Periodic Calculations

Xavier Solans-Monfort,[†,‡] Mariona Sodupe,*[,†] Vicenç Branchadell,[†] Joachim Sauer,[§] Roberto Orlando,[||] and Piero Ugliengo[⊥,#]

Departament de Quimica, Universitat Autonoma de Barcelona, Bellaterra, 08193, Spain, Institut für Chemie, Humboldt Universität zu Berlin, Berlin, D-10099, Germany, Dipartimento di Scienze e Tecnologie Avanzate, Università del Piemonte Orientale, C.so Borsalino 54, 15100 Alessandria, Italy, Dipartimento di Chimica IFM, Università di Torino, Via P. Giuria 7, 10125-Torino, Italy, and NIS—Nanostructured Interfaces and Surfaces—Centre of Excellence, c/o Dipartimento di Chimica IFM, Via Pietro Giuria 7, I-10125 Torino, Italy

Received: October 1, 2004; In Final Form: December 10, 2004

The adsorption of NH_3 and H_2O in acidic chabazite has been studied with the B3LYP method within the cluster approach (5T, 48T clusters) and the periodic approach adopting a Si/Al = 11/1 chabazite and a basis set of polarized double-ζ quality. The 5T cluster has been treated fully ab initio at the B3LYP level whereas the 48T cluster has been treated with the ONIOM2 scheme using B3LYP as the high level of theory and the MNDO, AM1, and HF/3-21G methods as low levels of theory. Periodic calculations show that the adsorption of NH_3 in acidic chabazite takes place through an ion pair ($NH_4^+-CHA^-$) structure, the computed adsorption energy being −32 kcal/mol. The adsorption of H_2O leads to a hydrogen bonded ($H_2O-HCHA$) complex with the computed adsorption energy of −20 kcal/mol. All ONIOM combinations provide similar structures to those obtained with periodic calculations. Adsorption energies, however, are sensitive to the low level used, especially for NH_3. The ONIOM B3LYP:HF/3-21G method is the one that provides more satisfactory results. Present results show that, for larger zeolites, the ONIOM scheme can be successfully applied while drastically reducing the cost of a fully ab initio treatment.

I. Introduction

Nowadays, zeolites are one of the most important heterogeneous catalysts, especially the proton exchanged ones due to their activity in acid−base catalysis.[1−4] Because of that, the knowledge and understanding of the acidic properties of Brønsted acid sites is a subject of great interest. Zeolite acidity is analyzed from indirect measurements,[5,6] for example by the adsorption of different probe molecules and the subsequent analysis of the adsorbed complexes and adsorption energy. Several techniques such as IR[7−14] and NMR[8,14−16] spectroscopies and temperature-programmed desorption[11−18] and microcalorimetry experiments[14,19−21] have been used on this purpose.

Among the large variety of probe molecules employed, ammonia has been one of the most widely used.[5,6,8,11−21] and its interaction with different zeolite frameworks is well-known. It has been reported that ammonia is basic enough to deprotonate proton exchanged zeolites forming an ion-pair (IP) structure, $NH_4^+-Z^-$.[8,11−13,16] Moreover, its adsorption energy at coverage of one probe molecule per active site has been estimated to lie between −26 and −38 kcal/mol depending on the zeolite structure and composition.[6,18−23] It is worth noting that the higher adsorption energies are usually related to frameworks with small channels and cavities.[6,23] The interaction of water molecules with acidic zeolite sites is also quite well-known as it is present in many catalyzed reactions. It has been observed that when one water molecule interacts with a Brønsted site, H_2O is not basic enough to deprotonate the zeolite and thus, a hydrogen-bonded (HB) complex is formed, H_2O-HZ.[7,9,24] The measured adsorption energies lie between −12 and −20 kcal/mol.[22]

The first theoretical studies analyzing the adsorption of probe molecules with Brønsted acid sites appeared at the beginning of the past decade. Small free clusters were used[24−32] and the obtained results were not always satisfactory. They predicted the formation of HB complexes reasonably well but not the IP ones. Furthermore, adsorption energies were generally underestimated, the underestimation being more important for the IP structures. Afterward, more elaborated models such as embedded clusters were designed,[33−39] which led to accurate results for many systems. In addition, periodic calculations were also carried out for some systems.[33,37,40−45] However, accurate periodic calculations can be computationally very demanding because zeolites normally present large units cells with low symmetry due to the Si/Al substitution. This fact has encouraged several researchers to look for cost-effective approaches to model zeolites.

In this context, the ONIOM approach[46−48] is increasingly being used in material chemistry modeling,[49−59] since the local or active site of the system can be treated with this hybrid method at a high level of theory, whereas the remaining part can be considered at a much lower (and less expensive) level. Besides the ONIOM approach, there are independent imple-

* Corresponding author. E-mail: mariona@klingon.uab.es.
[†] Universitat Autonoma de Barcelona.
[‡] Present address LSDSMS UMR5636 (CNRS−UM2), Université Montpellier 2, 34095 Montpellier Cedex 05, France.
[§] Humboldt Universität zu Berlin.
[||] Università del Piemonte Orientale.
[⊥] Università di Torino.
[#] NIS—Nanostructured Interfaces and Surfaces—Centre of Excellence. Website: http://www.nis.unito.it.

10.1021/jp045531e CCC: $30.25
Published on Web 02/08/2005

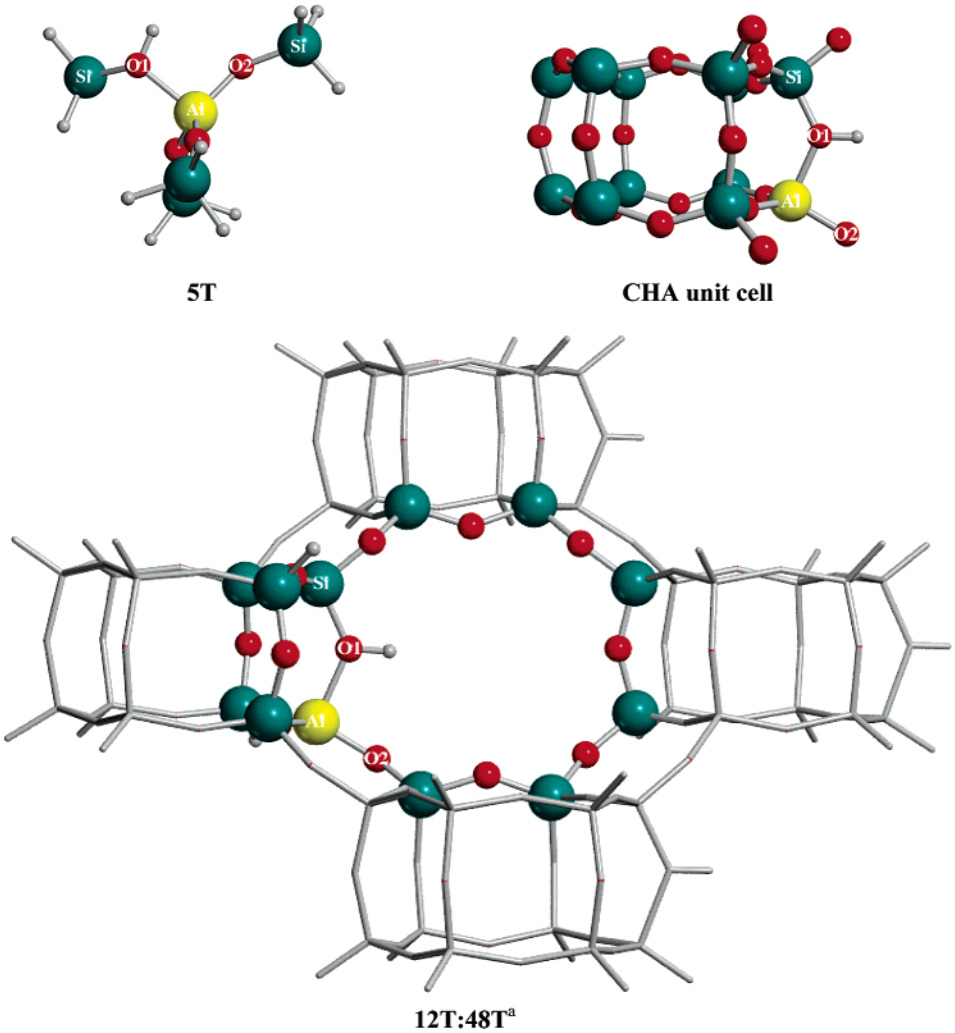

Figure 1. Chabazite unit cell and cluster models (5T and 12T:48T) used to study the adsorption of NH_3 and H_2O in chabazite. Footnote a: The region treated at the low level of theory with ONIOM2 is shown as tubes.

mentations of hybrid QM/QM methods, such us the MP2/plane wave DFT, that have also been applied in this field, for example, to study the adsorption of H_2O in acidic chabazite.[45]

The aim of the present study is to analyze the reliability of the ONIOM approach in the study of the NH_3 and H_2O adsorption in acidic chabazite, by comparing it with periodic calculations, other QM/MM results, and the available experimental data. For this purpose several combinations of different levels of theory as well as different partitions of the inner and outer layers have been considered. This study of water and ammonia adsorption will enable us to analyze the importance of the embedding effects in IP and HB complexes.

II. Computational Details

Three different strategies have been considered in modeling the zeolite. In the first the active site of the zeolite is represented by a pentatetrahedral cluster (5T) using a full ab initio approach. In the second a much larger cluster (48T) is considered with the hybrid two-layer ONIOM2 approach.[46−48] This 48 tetrahedra cluster is constructed from 4 unit cells, which define the eight-membered ring channel. The considered inner layer, treated at the higher level of calculation, has 12 tetrahedra (12T) formed by the inclusion of the eight-membered ring and the two four-membered ring around the Brønsted site. Hereafter, this cluster will be referred as 12T:48T. Because the 48 tetrahedra cluster extends far more than one cell, ONIOM calculations do not include the periodic images of H_2O and NH_3 that one would get if the cluster were cut out of the loaded chabazite structure. Finally, periodic ab initio calculations using localized basis sets based on Gaussian expansions of crystalline orbitals have been performed. Both for periodic and ONIOM cluster calculations the Si/Al ratio is set to 11/1. Figure 1 shows the 5T and the 12T:48T clusters as well as the chabazite unit cell.

Periodic ab initio simulations were performed using CRYSTAL03.[60] The Si/Al substitution reduces the symmetry of all-silica chabazite from the $R\bar{3}m$ space group to $P1$. The negative charge generated by the aluminum substitution is neutralized by adding a proton per unit cell (H−CHA). In all calculations the proton has been attached to the O1 position (see ref 61), since this site was found to be the most favored one. Unit cell parameters are fixed to those previously optimized for all silica chabazite.[62] Cell parameters are not relaxed to save computer resources, working under the hypothesis that this will not dramatically affect the adsorption energies of NH_3 and H_2O. Geometry optimizations of the fractional coordinates of all atoms belonging to the unit cell are performed using the algorithm implemented in the CRYSTAL03 code, which has been described elsewhere.[63−66] Present periodic calculations have been performed by applying the same numerical criteria as in our previous study of the H_2 storage in Cu^+ exchanged chabazite, and thus, for more computational details, the reader is referred to this previous work.[67]

The nonlocal hybrid B3LYP[68−70] density functional has been used as the level of theory for 5T, periodic calculations and as high level in the ONIOM2 calculations. The basis set used is the same adopted in previous studies of chabazite and it is of double-ζ plus polarization quality (BSA).[67] To test the reliability of this basis set, for cluster models, we have also performed geometry optimizations using the Pople's 6-31++G(d,p)[71] basis set (BSB). Finally, three different low levels have been used in the ONIOM2 approach: the semiempirical MNDO[72] and AM1[73] methods and the ab initio HF/3-21G level of theory. It should be noted that geometry optimizations of the 48T structures with ONIOM2 are full.

Basis set superposition error (BSSE) has been evaluated through the counterpoise correction.[74] For the adsorption of ammonia, we have considered the ammonium cation (NH_4^+) and the negative framework (CHA^-), while for the adsorption of water, the counterpoise correction has been computed assuming H_2O molecule and HCHA fragments. Because of the fact that for NH_3 adsorption both fragments are charged, the computation of the basis set superposition error for periodic calculations is not feasible since an infinitely charged solid is created. In this case, the adsorption energy corrected for basis set superposition error has been obtained assuming the same counterpoise correction computed for the ONIOM 12T:48T system. This is justified because for H_2O−HCHA the computed counterpoise corrections with 12T:48T and periodic calculations are very similar. Finally, in the ONIOM calculations, the counterpoise correction has only been computed for the inner layer. Molecular calculations have been carried out with the Gaussian 98 system package.[75]

III. Results and Discussion

Adsorption of NH_3. Figure 2 presents the optimized geometries of the adsorbed complexes obtained with all considered models. The NH_3 adsorption energies are given in Table 1. The ONIOM2 adsorption energies have been decomposed into two terms: the high level (HL) and the low level (LL), respectively. The HL term corresponds to the adsorption energy considering only the inner layer (12T) at the high level of theory, whereas the LL one indicates the correction introduced upon enlarging the cluster from 12T to 48T (see Table 1 for the definition of the LL term.)

Both the IP and HB complexes are found to be minima with the 5T cluster, the two structures being nearly degenerate and differing by 0.2 kcal/mol only. The IP complex presents two strong hydrogen bonds between the protons of ammonium ion and the oxygen atoms bonded to aluminum. The HB structure also presents two hydrogen bonds: one between the proton of the Brønsted site and the N of ammonia and the other one between a proton of NH_3 and an oxygen atom of the zeolite framework; of the two the former is stronger than the latter. For the IP structure the counterpoise corrected adsorption energy is −19.6 kcal/mol, only 0.2 kcal/mol more stable than the HB structure.

In contrast, when periodic calculations are performed, only the ion pair $NH_4^+CHA^-$ structure is found to be a minimum and the computed adsorption energy is −31.9 kcal/mol. The formation of an ion pair is in agreement with the experimental IR spectra, which show a large decrease of the band at ∼3600 cm^{-1}, associated with the Brønsted site, and the formation of characteristic bands in the 1350−1550 cm^{-1} range corresponding to the NH_4^+ cation.[8,11,13] Figure 2 shows that the ammonium ion is located in the eight-membered ring forming three hydrogen bonds with oxygen atoms of the zeolite framework, among which only one involves an oxygen atom bonded to aluminum. As expected, this latter hydrogen bond is at a shorter distance (1.62 Å) than the other two (1.96 and 2.61Å), due to the larger basicity of the oxygen atoms bonded to aluminum. This structure is more stable than the one with two hydrogen bonds involving oxygen atoms bonded to the same Al (as found with 5T), because in this case a higher geometrical strain is

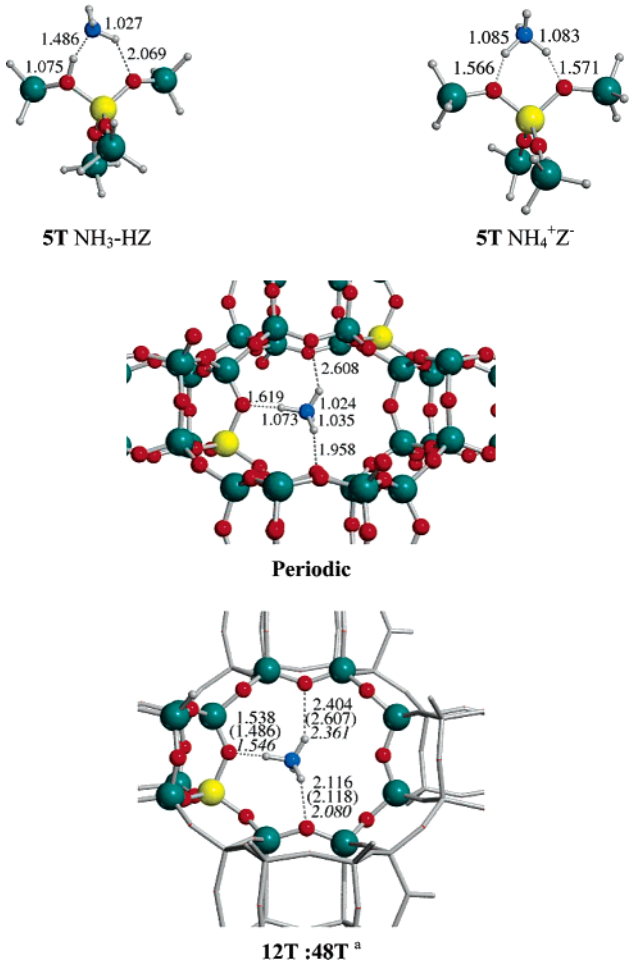

Figure 2. NH_3−HZ optimized structures at the B3LYP/BSA level of theory. (Distances are in Å). Footnote a: ONIOM2 results using B3LYP/BSA as high level and MNDO, (AM1) or *HF* methods as low level.

TABLE 1: NH_3 Adsorption Energies[a] (in kcal/mol) with Respect to the HZ + NH_3 Asymptote

model	method	E_{ads}	HL[b]	LL[c]
5T[d]	B3LYP/BSA	−24.2 (−19.6)		
12T:48T	B3LYP/BSA:MNDO	−32.5 (−27.5)	−32.1	−0.4
	B3LYP/BSA:AM1	−28.9 (−24.1)	−31.2	+2.3
	B3LYP/BSA:HF/3-21G	−34.8 (−29.9)	−31.6	−3.2
	B3LYP/BSA:HF/3-21G[e]	−35.0 (−30.0)	−32.1	−2.9
periodic	B3LYP/BSA	−36.9 (−31.9)[f]		
5T	B3LYP/BSB	−19.5 (−17.6)		
12T:48T	B3LYP/BSB:MNDO	−28.3 (−26.3)	−27.8	−0.5
	B3LYP/BSB:AM1	−25.1 (−23.1)	−27.3	+2.2
	B3LYP/BSB:HF/3-21G	−31.0 (−28.8)	−28.0	−3.0
	B3LYP/BSB:HF/3-21G[e]	−31.3 (−29.3)	−27.8	−3.5

[a] In parentheses are given the counterpoise corrected values. [b] High level contribution. HL = $E_{12T}^{high}(NH_4^+Z^-) - E^{high}(NH_3) - E_{12T}^{high}(HZ)$. [c] Low level contribution. LL = $E_{48T}^{low}(NH_4^+Z^-) - E_{12T}^{low}(NH_4^+Z^-) - [E_{48T}^{low}(HZ) - E_{12T}^{low}(HZ)]$. [d] Results correspond to the ion-pair structure. [e] Single point calculations at the B3LYP:MNDO optimized geometries. [f] Counterpoise corrected value was estimated. See text.

incorporated in the structure. A similar complex with three hydrogen bonds has been reported in the literature with periodic calculations at the Hartree−Fock level.[33,37] However, at this level of theory the adsorption energy is underestimated by about 25%, which points out the importance of including electron correlation effects.

The comparison between periodic and 5T results with the available experimental data reveals that 5T model does not describe the NH_3 adsorption properly, since it predicts the formation of a HB structure, which has not been observed experimentally.[8,11,13] Moreover, the computed adsorption energy with the 5T cluster (−19.6 kcal/mol) is much smaller (in absolute value) than that obtained with periodic calculations (−31.9 kcal/mol) or the experimental data (between −26 and −38 kcal/mol).[6,18−23] However, periodic calculations at the B3LYP/BSA level of theory provide a good description of the ion pair nature of the interaction and a reasonable value of the adsorption energy. The present periodic results will be taken as reference to evaluate the performance of the ONIOM2 approach.

As mentioned in the Introduction, an important goal of this work is to test the reliability of the ONIOM approach in modeling adsorption processes in acidic zeolites. In particular, it is important to analyze if the inclusion of the eight-member ring, where the adsorption takes place, with appropriate geometry constraints is sufficient to correct the deficiencies of small clusters. Results have shown that ONIOM optimizations of a 12T:48T cluster lead to the formation of the IP structure, NH_4^+−CHA^-, regardless of the low level method used to describe the real system. It should be noticed that all optimizations have been performed without freezing any degree of freedom, at variance with other studies in which the structures have been optimized partially.[56−58] The possible formation of the HB structure, NH_3−HCHA, has been explored at the B3LYP/BSA:MNDO level but all our attempts evolved to the ion pair complex. As found for periodic calculations, NH_4^+ lies in the eight-membered ring with three of its protons pointing to three oxygen atoms of the ring (see Figure 2), the shortest bond being with the oxygen atom bonded to Al. The other two O···H distances are always larger than 2 Å, and the hydrogen bond interaction is expected to be relatively small. Overall, all of the ONIOM combinations lead to very similar structures around the active site, the larger variations being observed, not unexpectedly, for the weaker H-bonds. Thus, all considered low levels impose similar constraints.

The computed ONIOM adsorption energies with the 12T:48T cluster lie between the values obtained for 5T and periodic calculations and significantly depend on the low level of theory used. The use of AM1 and MNDO semiempirical methods as low level leads to a weaker interaction (−24.1 and −27.5 kcal/mol, respectively) than that computed with the B3LYP:HF (−29.9 kcal/mol) or periodic B3LYP (−31.9 kcal/mol). The decomposition of the adsorption energy into the high level (HL) and low level (LL) contributions shows that the HL term is very similar in all ONIOM2 combinations, which indicates that the geometry differences of the inner part do not affect the adsorption energy and that all low-levels used introduce similar geometry constraints due to the zeolite framework. The differences in the adsorption energy mainly arise from the low level contribution, the result from the B3LYP/BSA:HF/3-21G combination best matches with the periodic reference value.

It must be pointed out that ONIOM2(B3LYP/BSA:HF/3-21G) optimizations are computationally expensive and thus, the ONIOM approach does not represent an important computational gain compared to the periodic calculation. Considering that all low levels lead to similar geometry constraints, we tested the reliability of performing single point B3LYP/BSA:HF/3-21G calculations at the B3LYP/BSA:MNDO geometries. We have taken B3LYP/BSA:MNDO geometries since Roggero et al.[49] showed that MNDO is the semiempirical method that leads to zeolite geometry parameters closer to the experimental ones. Remarkably, the results (Table 1) are within 0.5 kcal/mol of those computed at the B3LYP/BSA:HF/3-21G optimized geometries, while the computational cost is much lower. Consequently, the use of B3LYP/BSA:HF/3-21G//B3LYP/BSA:MNDO approach seems to be a good strategy to model this kind of systems, particularly for zeolites with very large unit cells as in ZSM5.

To analyze the effect of further enlarging the basis set, we have also performed B3LYP/BSB optimizations for the 5T and 12T:48T clusters. The computed adsorption energies have been included in Table 1. While geometry parameters change only slightly upon increasing the basis set, the adsorption energies decrease considerably. This decrease mainly arises from the High Level contribution. However, when the energy is corrected for BSSE the obtained results are very similar. This indicates that, although the small BSA leads to too high interaction energies, they are reasonably corrected when the counterpoise correction is added.

Finally, we have analyzed the importance of the inner and outer layer partition by constructing ONIOM clusters with different inner layer size. Figure 3 shows the optimized structures of the adsorbed complexes with B3LYP:MNDO, while Table 2 presents the adsorption energies obtained using both the B3LYP/BSA:MNDO and the B3LYP/BSA:HF/3-21G combinations. It can be observed that the clusters with smaller inner layers (5T:48T and 8T:48T) lead to an interaction between NH_4^+ and the zeolite framework similar to that observed for free 5T; that is, in all cases analyzed two short hydrogen bonds are formed with oxygens bonded to Al. This is due to the absence of other oxygen atoms of the ring framework zeolite in the inner layer. When the inner layer is enlarged to 10T:48T, the adsorbed complex presents three hydrogen bonds, similar to what is observed in periodic calculations. This is not surprising considering that the 10T:48T cluster already includes in the inner layer all the oxygen atoms needed to form the three hydrogen bonds found with the periodic approach. Further enlargements of the inner layer size produce little changes in the geometry of the adsorbed complex. Consequently, the inclusion of all the oxygens involved in hydrogen bonds is necessary to get a proper description of the interaction and defines the minimum size of the inner layer in the ONIOM partition. This fact is in line with the general recipe at any ONIOM calculations, i.e., the inner zone should include all atoms relevant for the chemical process taking place in the considered system.

With respect to the adsorption energies (Table 2), it is observed that B3LYP/BSA:MNDO absolute values increase as the inner layer is enlarged. This is mainly due to the HL term, which increases with the size of the inner layer. The LL contribution, however, shows an almost erratic behavior. On the other hand, single point B3LYP/BSA:HF/3-21G//B3LYP/BSA:MNDO adsorption energies are always similar regardless of the layer partition, given that the increase of the HL term with the cluster size is compensated with a similar decrease of the low level contribution. This indicates that HF/3-21G is by far the most appropriate low level method in agreement with the results reported for the NH_3 adsorption on silica cluster model.[49]

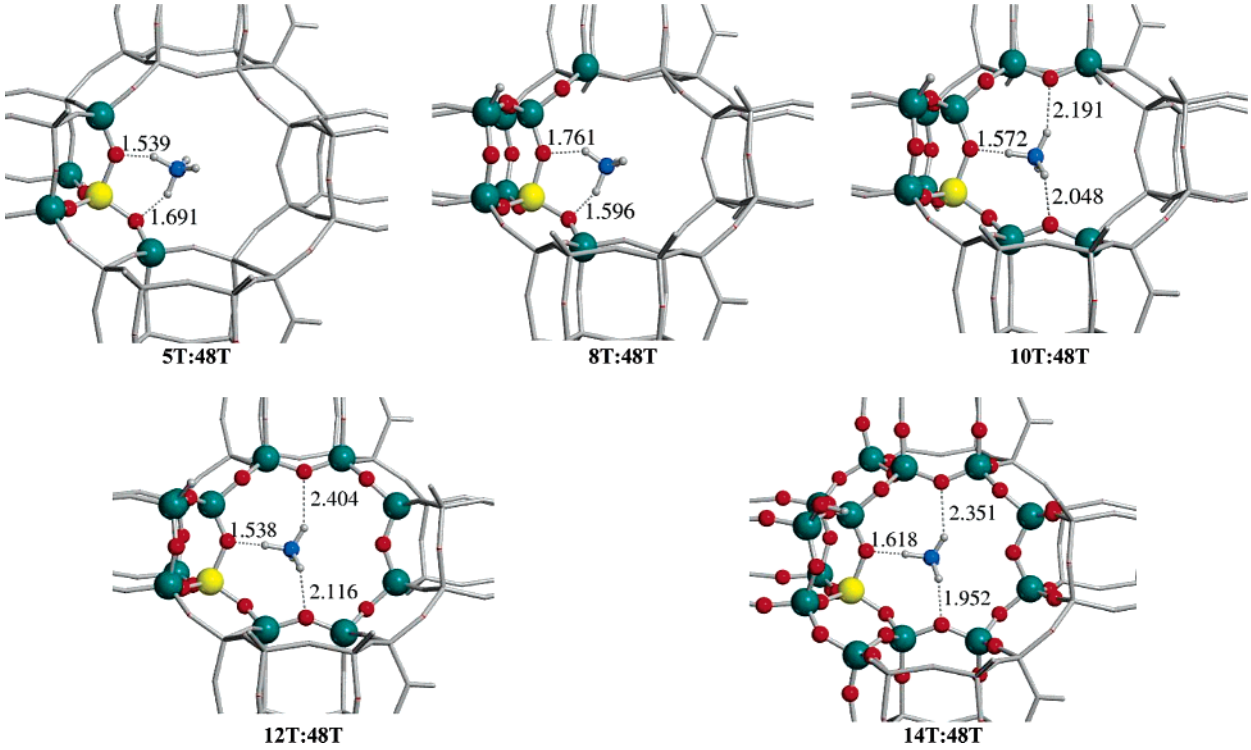

Figure 3. ONIOM2 optimized geometries of $NH_4^+-Z^-$, using the B3LYP/BSA:MNDO methods combination and different layer partitions. (Distances are in Å.)

TABLE 2: ONIOM2 Adsorption Energies[a] (in kcal/mol) with Respect to the HZ + NH_3 Asymptote

	B3LYP/BSA:MNDO			B3LYP/BSA:HF/3-21G[b]		
*x*T:48T	E_{ads}	HL[c]	LL[d]	E_{ads}	HL[c]	LL[d]
5T:48T	−22.9 (−18.4)	*−24.1*	*+1.2*	−35.4 (−31.0)	*−24.1*	*−11.3*
8T:48T	−29.6 (−25.2)	*−24.3*	*−5.3*	−32.3 (−27.8)	*−24.3*	*−8.0*
10T:48T	−34.2 (−30.0)	*−30.1*	*−4.1*	−33.7 (−29.3)	*−30.1*	*−3.6*
12T:48T	−32.5 (−27.5)	*−32.1*	*−0.4*	−35.0 (−30.0)	*−32.1*	*−2.9*
14T:48T	−36.9 (−32.1)	*−32.8*	*−4.1*	−33.4 (−28.6)	*−32.8*	*−0.6*

[a] In parentheses are given the counterpoise corrected values. [b] Single point calculations at the B3LYP/BSA:MNDO optimized geometries. [c] High level contribution. HL = $E_{xT}^{high}(NH_4^+Z^-) - E^{high}(NH_3) - E_{xT}^{high}(HZ)$. [d] Low level contribution. LL = $E_{48T}^{low}(NH_4^+Z^-) - E_{xT}^{low}(NH_4^+Z^-) - [E_{48T}^{low}(HZ) - E_{xT}^{low}(HZ)]$.

In summary, present results indicate that the inclusion of the oxygen atoms that might be involved in the hydrogen bonds as well as the eight-membered ring in the high level region is important to accurately describe the adsorption of NH_3 in HCHA. The addition of the channel atoms where the adsorption takes place gives extra-stabilization due to the lone pairs of zeolite O atoms pointing toward the positive charge of the ammonium ion. On the other hand, the good agreement between 12T:48T cluster and periodic calculations shows that the size considered for the full system in ONIOM2 calculations (48T) is very appropriate and that the effect of the remaining solid framework is small. Although we have not analyzed the importance of the size of the full system, results with smaller clusters will probably lead to too distorted structures in such a way that the structural similarity with the original material (chabazite) will be lost. Present results show that well tested ONIOM clusters will show a high accuracy/cost ratio in modeling processes in acidic zeolites characterized by very large unit cells.

Another hybrid method, the QM-Pot embedded cluster method,[76,77] has provided very similar results for NH_3 adsorption in H−Chabazite.[37,39] As with the present ONIOM calculations, an NH_4^+ ion with three protons pointing to O atoms of the framework has been found to be the most stable in structure optimizations of an 8-ring model embedded in a periodic environment.[37] This was done at the Hartree−Fock level, but electron correlation effects have been included by single point MP2 calculations on a 3T cluster. The (BSSE corrected) adsorption energy obtained (−30.6 kcal/mol)[39] is between the periodic calculation (−31.9 kcal/mol) and the B3LYP/BSB:HF/3-21G ONIOM result (−29.3 kcal/mol).

Adsorption of H_2O. Figure 4 shows the optimized geometries of the adsorbed complexes obtained with all considered zeolite models, and Table 3 shows the H_2O adsorption energies, which again have been decomposed into the high level (HL) and low level (LL) terms.

Calculations with the 5T cluster lead to a H_2O−HZ hydrogen bonded structure. Two hydrogen bonds are formed, one between the proton of the zeolite Brønsted site and the O of water, and the second one between a proton of the water molecule and the oxygen atom bonded to Al. The adsorption energy, after correcting for BSSE, is −17.1 kcal/mol, well within the experimental range (−12 to −20 kcal/mol)[22] and in good agreement with previous theoretical studies based on free cluster models.[29−31,78] In agreement with the cluster results, periodic calculations also lead to a hydrogen bonded complex with a similar hydrogen bond pattern. However, in contrast to 5T, the hydrogen bond in which water acts as proton donor takes place with an oxygen atom not bonded to Al. The computed interaction energy is −20.0 kcal/mol in good agreement with the experimental data. Similar conclusions and adsorption energies were obtained for the H_2O adsorption in other zeolite frameworks using periodic calculations with GGA functionals and plane waves.[40−45]

ONIOM calculations using B3LYP/BSA:MNDO with the 12T:48T cluster lead to a geometry similar to that obtained with periodic calculations. The adsorption energy (−20.3 kcal/mol), computed from B3LYP/BSA:HF/3-21G single point calculations

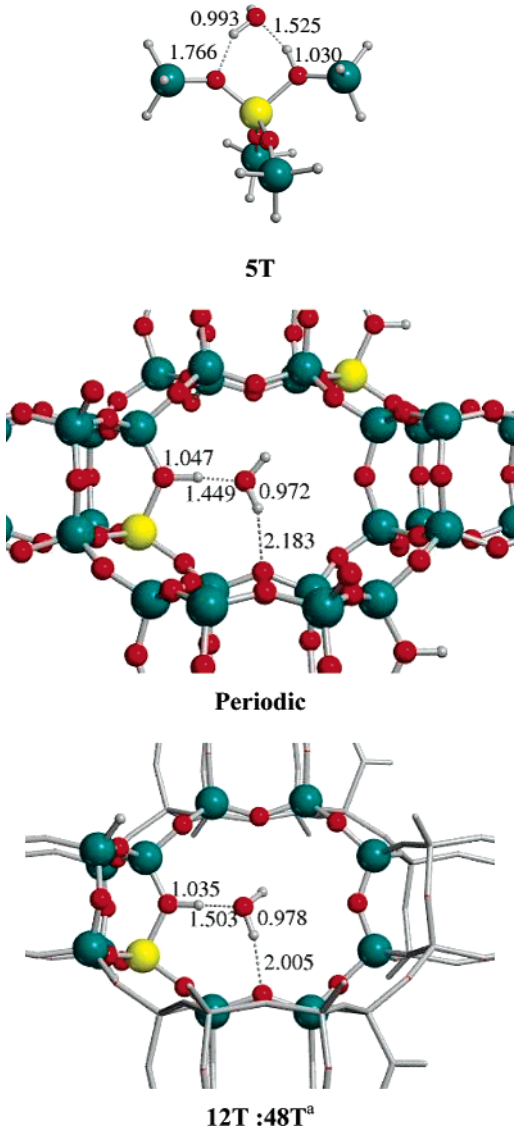

Figure 4. H_2O−HZ optimized structures at the B3LYP/BSA level of theory. (Distances are in Å.) Footnote a: ONIOM2 results using the B3LYP/BSA:MNDO methods combination.

TABLE 3: H_2O Adsorption Energies[a] (in kcal/mol)

model	method	E_{ads}	HL[b]	LL[c]
5T	B3LYP/BSA	−23.2 (−17.1)		
12T:48T	B3LYP/BSA:MNDO	−26.1 (−19.5)	−26.2	+0.1
	B3LYP/BSA:HF/3-21G[d]	−26.9 (−20.3)	−26.2	−0.7
periodic		−26.4 (−20.0)		

[a] In parentheses are given the counterpoise corrected values. [b] High level contribution. HL = $E_{12T}^{high}(H_2OHZ) - E^{high}(H_2O) - E_{12T}^{high}(HZ)$. [c] Low level contribution. LL = $E_{48T}^{low}(H_2OHZ) - E_{12T}^{low}(H_2OHZ) - [E_{48T}^{low}(HZ) - E_{12T}^{low}(HZ)]$. [d] Single point calculations at the B3LYP/BSA:MNDO optimized geometries.

at the B3LYP/BSA:MNDO optimized geometries, is also in excellent agreement with the periodic value. The decomposition into the HL and LL terms show that the LL contribution is much smaller than for the ammonia case, showing that long-range forces are more important in the IP system. Furthermore, since the low level contribution is smaller, the B3LYP/BSA:MNDO (−19.5 kcal/mol) adsorption energy is also close to the periodic value.

Other hybrid approaches, such as the QM-pot embedded cluster method,[76,77] have also provided very good results for the H_2O adsorption in acidic chabazite.[79] Recent calculations at the B3LYP level with a triple-ζ plus polarization quality basis set, using a 14T cluster for the quantum mechanical part, provide an adsorption energy of −26.1 kcal/mol, in very good agreement with the value computed from the present periodic calculations without correcting for basis set superposition error.

In conclusion, for H_2O and probably for probe molecules that form neutral hydrogen bond complexes, the differences between different inner zones in the zeolite are smaller than when an ion pair is involved. This fact is due to the absence of net charges in the inner zone which give rise to long-range interactions extending also in the real system. However, some limitations are still observed with small clusters such as 5T given that the adsorption energies are somewhat underestimated and the obtained structure is not the global minimum inside the whole framework.

IV. Conclusions

The adsorption of NH_3 and H_2O on acidic chabazite has been studied using three different approaches to model the zeolite, a pentatetrahedral 5T cluster, a 12T:48T cluster with the two layer ONIOM2 method, and periodic calculations. Periodic calculations show that the adsorption of NH_3 in acidic chabazite takes place through an ion pair structure ($NH_4^+CHA^-$). The ammonium ion is located in the eight-member ring and forms three hydrogen bonds with oxygens of the zeolite framework. Our best estimated value for the adsorption energy is −32 kcal/mol. For the adsorption of H_2O, a hydrogen bonded system (H_2O−HCHA) is formed. The interaction takes place through two hydrogen bonds and the predicted adsorption energy is −20 kcal/mol. These results are in good agreement with the available experimental data for both systems.[6,22]

The less computationally demanding 5T cluster is not able to reproduce neither the adsorption structure nor the adsorption energy of NH_3 in chabazite. Nevertheless, for H_2O the structure and the adsorption energy obtained with the 5T cluster are better described than for NH_3. Overall, the 5T cluster is not reliable enough and larger clusters should be used.

ONIOM calculations with a 12T:48T cluster provide structures close to those computed with periodic calculations. However, adsorption energies, especially for the NH_3 system, do depend on the low level method used. The HF/3-21G as low level method is needed to reproduce the periodic binding energy, whereas semiempirical MNDO or AM1 provide too small interaction energies. The expensive B3LYP:HF/3-21G optimization can be avoided by performing single point calculations at the B3LYP:MNDO geometries. An analysis of the inner and outer layer partition show that the inner layer should include at least all the O atoms that might be involved in the local interaction between the guest and the zeolite, although the inclusion of the ring where the adsorption takes place allows for a more balanced description of all the relevant interactions including also the appropriate framework constraints. Finally, the good agreement between 12T:48T and periodic calculations suggest that the long-range effects are not extending too far even when ion pairs are involved.

Acknowledgment. Financial support from MCYT and FEDER (Project BQU2002-04112-C02) and DURSI (Project 2001SGR-00182) and the use of the computational facilities of the Catalonia Supercomputer Center (CESCA) are gratefully acknowledged. X.S.-M. acknowledges the Generalitat the Catalunya for a mobility grant and the group of Prof. Zecchina for a Marie Curie Training Site grant.

References and Notes

(1) Hölderich, W.; Hesse, M.; Näumann, F. *Angew. Chem., Int. Ed. Engl.* **1988**, *27*, 226.
(2) Corma, A. *Chem. Rev.* **1995**, *95*, 559.
(3) Sen, S. E.; Smith, S. M.; Sullivan, K. A. *Tetrahedron* **1999**, *55*, 12657.
(4) Ghobarkar, H.; Schäf, O.; Guth, U. *Prog. Solid St. Chem.* **1999**, *27*, 29.
(5) Valyon, J. Onyestyák, G.; Rees, L. V. C. *J. Phys. Chem. B* **1998**, *102*, 8994.
(6) Farneth, W. E.; Gorte, R. J. *Chem. Rev.* **1995**, *95*, 615.
(7) Zecchina, A.; Geobaldo, F.; Spoto, G.; Bordiga, S.; Ricchiardi, G.; Buzzoni, R.; Petrini, G. *J. Phys. Chem.* **1996**, *100*, 16584.
(8) Yin, F.; Blumenfeld, A. L.; Gruver, V.; Fripiat, J. J. *J. Phys. Chem. B* **1997**, *101*, 1824.
(9) Pazé, C.; Bordiga, S.; Lamberti, C.; Salvalaggio, M.; Zecchina, A.; Bellussi, G. *J. Phys. Chem. B* **1997**, *101*, 4740.
(10) Paukshtis, E. A.; Malysheva, L. V.; Stepanov, V. G. *React. Kinet. Catal. Lett.* **1998**, *65*, 145.
(11) Barthos, R.; Lónyi, F.; Onyestyák, G.; Valyon, J. *J. Phys. Chem. B* **2000**, *104*, 7311.
(12) Lónyi, F.; Valyon, J. *Thermochim. Acta* **2001**, *373*, 53.
(13) Lónyi, F.; Valyon, J. *Microporous Mesoporous Mater.* **2001**, *47*, 293.
(14) Boréave, A.; Auroux, A.; Guimon, C. *Micropor. Mater.* **1997**, *11*, 275.
(15) Kao, H.-M.; Grey, C. P. *J. Phys. Chem.* **1996**, *100*, 5105.
(16) Jacobs, W. P. J. H.; de Haan, J. W.; van de Ven, L. J. M.; van Santen, R. A. *J. Phys. Chem.* **1993**, *97*, 10394.
(17) Kapustin, G. I.; Brueva, T. R. *Thermochim. Acta* **2001**, *379*, 71.
(18) Katada, N.; Igi, H.; Kim, J.-H.; Niwa, M. *J. Phys. Chem. B* **1997**, *101*, 5969.
(19) Brueva, T. R.; Mishin, I. V.; Kapustin, G. I. *Thermochim. Acta* **2001**, *379*, 15.
(20) Parrillo, D. J.; Gorte, R. J. *J. Phys. Chem.* **1993**, *97*, 8786.
(21) Lee, C.; Parrillo, D. J.; Gorte, R. J.; Farneth, W. E. *J. Am. Chem. Soc.* **1996**, *118*, 3262.
(22) Sauer, J.; Ugliengo, P.; Garrone, E.; Saunders, V. R. *Chem. Rev.* **1994**, *94*, 2095.
(23) Auroux, A. *Top. Catal.* **1997**, *4*, 71.
(24) Jobic, H.; Tuel, A.; Krossner, M.; Sauer, J. *J. Phys. Chem.* **1996**, *100*, 19545.
(25) Zygmunt, S. A.; Brand, H. V.; Lucas, D. J.; Iton, L. E.; Curtis, L. A. *J. Mol. Struct.: THEOCHEM* **1994**, *314*, 113.
(26) Teunissen, E. H.; van Santen, R. A.; Jansen, A. P. J.; van Duijneveldt, F. B. *J. Phys. Chem.* **1993**, *97*, 203.
(27) Kassab, E.; Fouquet, J.; Allavena, M.; Evleth, E. M. *J. Phys. Chem.* **1993**, *97*, 9034.
(28) Pelmenschikov, A. G.; van Santen, R. A. *J. Phys. Chem.* **1993**, *97*, 10678.
(29) Zygmunt, S. A.; Curtiss, L. A.; Iton, L. E.; Erhardt, M. K. *J. Phys. Chem.* **1996**, *100*, 6663.
(30) Krossner, M.; Sauer, J. *J. Phys. Chem.* **1996**, *100*, 6199.
(31) Ryder, J. A.; Chakraborty, A. K.; Bell, A. T. *J. Phys. Chem. B* **2000**, *104*, 6998.
(32) Zygmunt, S. A.; Curtiss, L. A.; Iton, L. E. *J. Phys. Chem. B* **2001**, *105*, 3034.
(33) Teunissen, E. H.; Jansen, A. P. J.; van Santen, R. A.; Orlando, R.; Dovesi, R. *J. Chem. Phys.* **1994**, *101*, 5865.
(34) Teunissen, E. H.; Jansen, A. P. J.; van Santen, R. A. *J. Phys. Chem.* **1995**, *99*, 1873.
(35) Kyrlidis, A.; Cook, S. J.; Chakraborty, A. K.; Bell, A. T.; Theodorou, D. N. *J. Phys. Chem.* **1995**, *99*, 1505.
(36) Vollmer, J. M.; Stefanovich, E. V.; Truong, T. N. *J. Phys. Chem. B* **1999**, *103*, 9415.
(37) Brändle, M.; Sauer, J.; Dovesi, R.; Harrison, N. M. *J. Chem. Phys.* **1998**, *109*, 10379.
(38) Sierka, M.; Sauer, J. *J. Phys. Chem. B* **2001**, *105*, 1603.
(39) Brändle, M.; Sauer, J. *J. Am. Chem. Soc.* **1998**, *120*, 1556.
(40) Nusterer, E.; Blöchl, P. E.; Schwarz, K. *Chem. Phys. Lett.* **1996**, *253*, 448.
(41) Benco, L.; Demuth, Th., Hafner, J.; Hutschka, F. *Chem. Phys. Lett.* **2000**, *324*, 373.
(42) (a) Jeanvoine, Y.; Ángyán, J. G.; Kresse, G.; Hafner, J. *J. Phys. Chem. B* **1998**, *102*, 7307. (b) Termath, V.; Haase, F.; Sauer, J.; Hutter, J.; Parrinello, M. *J. Am. Chem. Soc.* **1998**, *120*, 8512.
(43) Demuth, Th.; Benco, L.; Hafner, J.; Toulhoat, H. *Int. J. Quantum Chem.* **2001**, *84*, 110.
(44) Lo, C.; Trout, B. L. *J. Catal.* **2004**, *227*, 77.
(45) Tuma, C.; Sauer, J. *Chem. Phys. Lett.*. **2004**, *387*, 388.
(46) Maseras, F.; Morokuma, K. *J. Comput. Chem.* **1995**, *16*, 1170.
(47) Vreven, T.; Morokuma, K. *J. Comput. Chem.* **2000**, *21*, 1419.
(48) Dapprich, S.; Komáromi, I.; Byun, K. S.; Morokuma, K. Frisch, M. J. *J. Mol. Struct. (THEOCHEM)* **1999**, *461*, 1.
(49) Roggero, I.; Civalleri, B.; Ugliengo, P. *Chem. Phys. Lett.* **2001**, *341*, 625.
(50) Erbetta, D.; Ricci, D.; Pacchioni, G. *J. Chem. Phys.* **2000**, *113*, 10744.
(51) Raksakoon, C.; Limtrakul, J. *J. Mol. Struct.: THEOCHEM* **2003**, *631*, 147.
(52) (a) Damin, A.; Bordiga, S.; Zecchina, A.; Lamberti, C. *J. Chem. Phys.* **2002**, *117*, 226. (b) Damin, A.; Bordiga, S.; Zecchina, A.; Doll, K.; Lamberti, C. *J. Chem. Phys.* **2003**, *118*, 10183. (c) Bonino, F.; Damin, A.; Bordiga, S.; Lamberti, C.; Zecchina, A. *Langmuir* **2003**, *19*, 2155.
(53) Lopez, N.; Pacchioni, G.; Maseras, F.; Illas, F. *Chem. Phys. Lett.* **1998**, *294*, 611.
(54) Solans-Monfort, X.; Bertran, J.; Branchadell, V.; Sodupe, M. *J. Phys. Chem. B* **2002**, *106*, 10220.
(55) Sillar, K.; Burk, P. *J. Mol. Struct.: THEOCHEM* **2002**, *589*−*590*, 281.
(56) Kasuriya, S.; Namuangruk, S.; Treesukol, P.; Tirtowidjojo, M.; Limtrakul, J. *J. Catal.* **2003**, *219*, 320.
(57) Bobuatong, K.; Limtrakul, J. *Appl. Catal., A: Gen.* **2003**, *253*, 49.
(58) Jiang, N.; Yuan, S.; Wang, J.; Jiao, H.; Qin, Z.; Li, Y.-W *J. Mol. Catal. A* **2004**, *220*, 221.
(59) Sillar, K.; Burk, P. *J. Phys. Chem. B* **2004**, *108*, 9893.
(60) Saunders, V. R.; Dovesi, R.; Roetti, C.; Orlando, R.; Zicovich-Wilson, C. M.; Harrison, N. M.; Doll, K.; Civalleri, B.; Bush, I. J.; D'Arco, Ph.; Llunell, M. CRYSTAL03, 2003 development version, available on the web at http://www.crystal.unito.it.
(61) Civalleri, B.; Ferrari, A. M.; Llunell, M.; Orlando, R.; Mérawa, M.; Ugliengo, P. *Chem. Mater.* **2003**, *15*, 3996.
(62) Pascale, F.; Ugliengo, P.; Civalleri, B.; Orlando, R.; D'Arco, P.; Dovesi, R. *J. Chem. Phys.* **2002**, *117*, 5337.
(63) Doll, K.; Saunders, V. R.; Harrison, N. M. *Int. J. Quantum Chem.* **2001**, *82*, 1.
(64) Doll, K. *Comput. Phys. Commun.* **2001**, *137*, 74.
(65) Civalleri, B.; D'Arco, Ph.; Orlando, R.; Saunders, V. R.; Dovesi, R. *Chem. Phys. Lett.* **2001**, *348*, 131.
(66) Schlegel, H. B. *J. Comput. Chem.* **1982**, *3*, 214.
(67) Solans-Monfort, X.; Branchadell, V.; Sodupe, M.; Zicovich-Wilson, C. M.; Gribov, E.; Spoto, G.; Busco, C.; Ugliengo, P. *J. Phys. Chem. B,* **2004**, *108*, 8278.
(68) Becke, A. D. *J. Chem. Phys.* **1993**, *98*, 5648.
(69) Lee, C.; Yang, W.; Parr, R. G. *Phys. Rev. B* **1988**, *37*, 785.
(70) Stephens, P. J.; Declin, F. J.; Chabalowski, C. F.; Frisch, M. J. *J. Phys. Chem.* **1994**, *98*, 11623.
(71) Hehre, W. J.; Ditchfield, R.; Pople, J. A. *J. Chem. Phys.* **1972**, *56*, 2257.
(72) Dewar, M. J. S.; Thiel, W. *J. Am. Chem. Soc.* **1977**, *99*, 4899.
(73) Dewar, M. J. S.; Zoebisch, E. G.; Healy, E. F.; Stewart, J. J. P. *J. Am. Chem. Soc.* **1985**, *107*, 3902.
(74) Boys, S. F.; Bernardi, F. *Mol. Phys.* **1970**, *19*, 553.
(75) Frisch, M. J.; Trucks, G. W.; Schlegel, H. B.; Scuseria, G. E.; Robb, M. A.; Cheeseman, J. R.; Zakrzewski, V. G.; Montgomery, J. A.; Stratmann, R. E.; Burant, J. C.; Dapprich, S.; Millam, J. M.; Daniels, A. D.; Kudin, K. N.; Strain, M. C.; Farkas, O.; Tomasi, J.; Barone; V.; Cossi, M.; Cammi, R.; Mennucci, B.; Pomelli, C.; Adamo, C.; Clifford, S.; Ochterski, J.; Petersson, G. A.; Ayala, P. Y.; Cui, Q.; Morokuma, K.; Malick, D. K.; Rabuck, A. D.; Raghavachari, K.; Foresman, J. B.; Cioslowski, J.; Ortiz, J. V.; Baboul, A. G.; Stefanov, B. B.; Liu, G.; Liashenko, A.; Piskorz, P.; Komaromi, I.; Gomperts, R.; Martin, R. L.; Fox, D. J.; Keith, T.; Head-Gordon, M.; Replogle, E. S.; Pople, J. A. *Gaussian 98*; Gaussian Inc.: Pittsburgh, 1998.
(76) Sierka, M.; Sauer, J. *J. Chem. Phys.* **2000**, *112*, 6983.
(77) Eichler, U.; Kölmel, C. M.; Sauer, J. *J. Comput. Chem.* **1997**, *18*, 463.
(78) Mihaleva, V. V.; van Santen, R. A.; Jansen, A. P. *J. Chem. Phys.* **2004**, *120*, 9212.
(79) Kerber, T.; Diploma Thesis, Humboldt-Universität zu Berlin, 2004.